

Figure S1

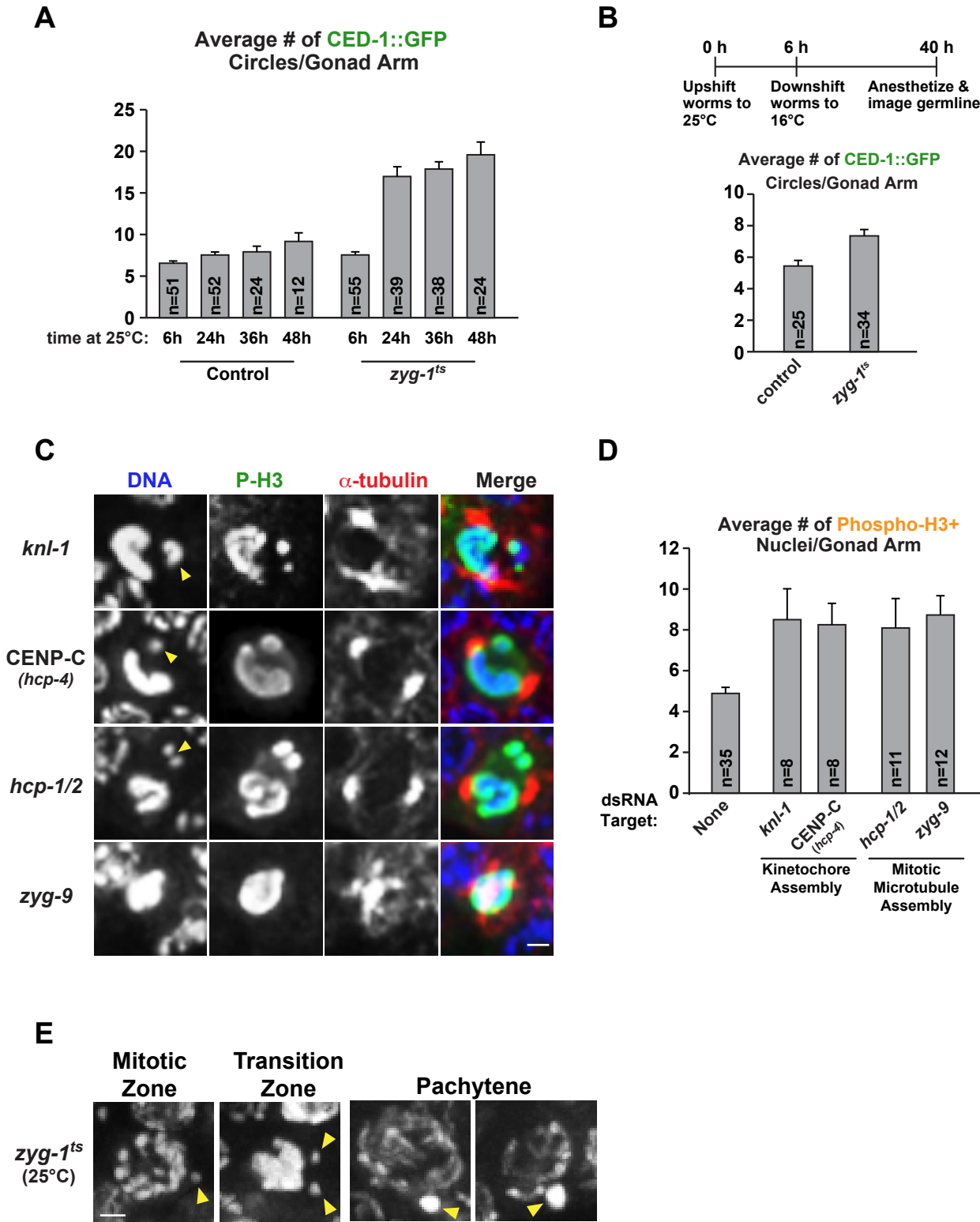


Figure S2

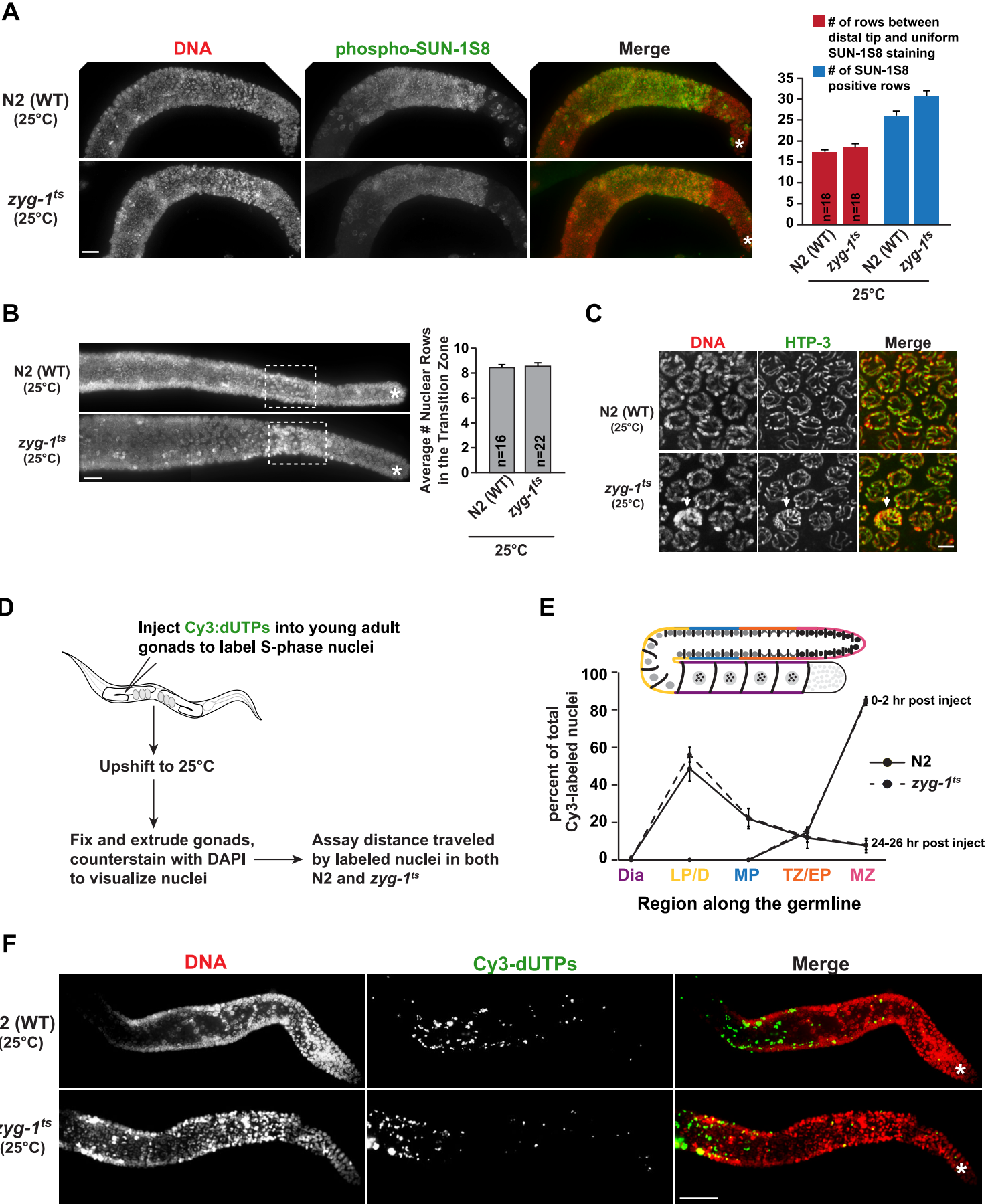
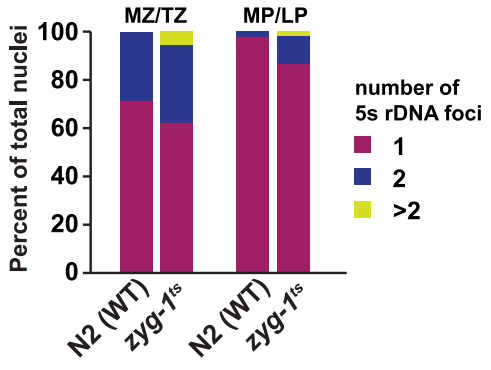
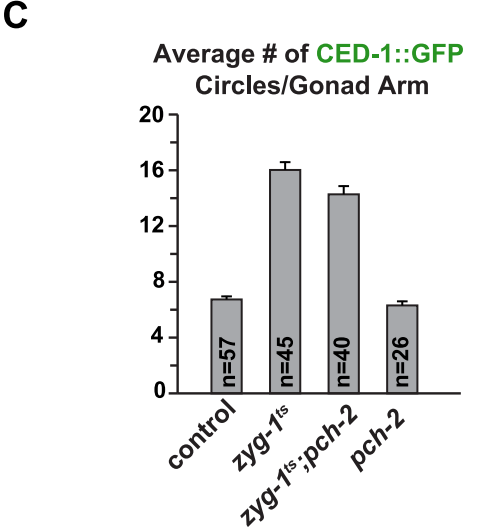
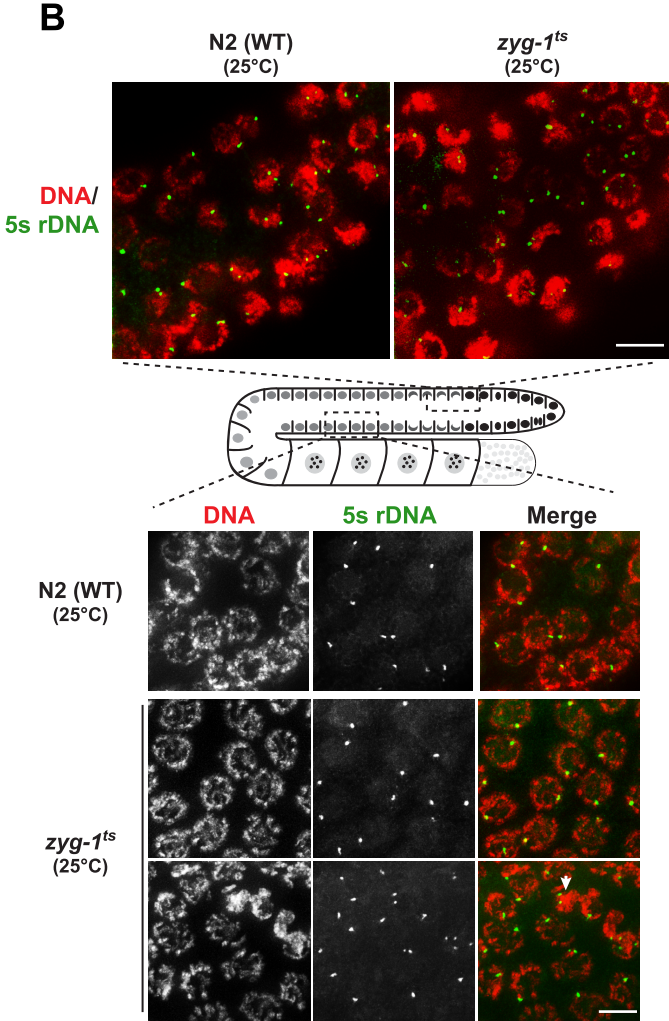
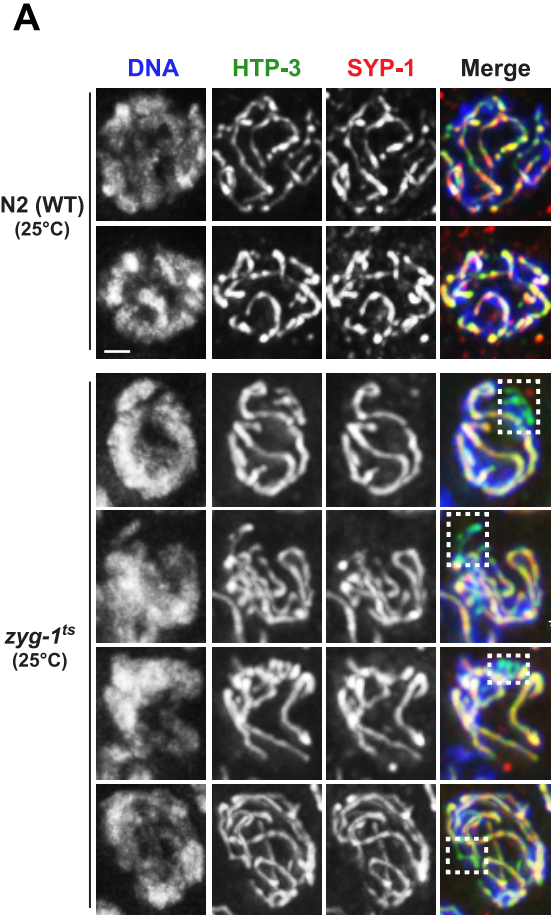
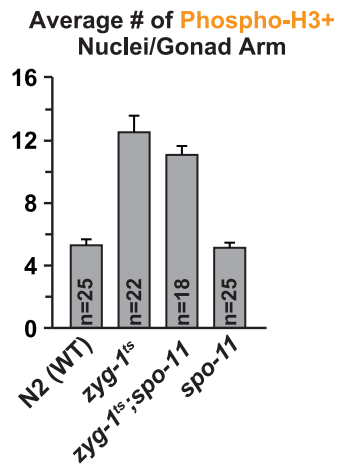


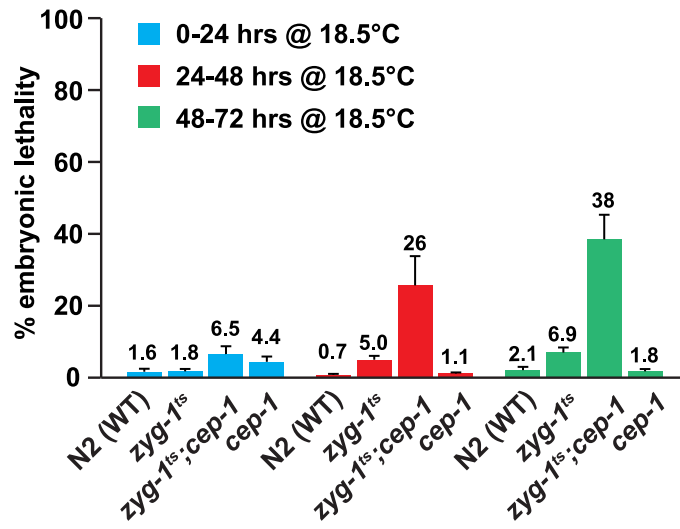
Figure S3



A



B



SUPPLEMENTAL FIGURE LEGENDS

Figure S1. Inhibition of mitosis results in defective nuclei that cause an increase in germline cell death.

(A) Quantification of each individual timepoint from the data presented in *Fig. 1C*. Each bar represents the average number of CED-1::GFP positive circles per condition. Error bars are SEM; one-way ANOVA analysis shows no significant difference between the 24, 36 and 48h time points for either control or *zyg-1^{ts}* ($p=0.23$ and $p=0.33$, respectively). The 6-hour upshift, which is adequate enough to inhibit centrosome duplication but does not allow enough time for nuclei from the mitotic zone to travel to the region of cell death, shows no significant difference (unpaired *t* test, $p=0.07$) between control and *zyg-1^{ts}*.

(B) Quantification of cell death seen upon recovery after upshift to chase the defective mitotic nuclei to the region of cell death; experimental regime is presented above the graph. Each bar represents the average number of CED-1::GFP positive circles. Error bars are SEM, unpaired *t* test shows a significant difference between control and *zyg-1^{ts}* worms, $p=0.0012$.

(C) Immunofluorescence images of the mitotic zone of extruded gonads stained with DAPI, α -tubulin and γ -tubulin for both the control and mitotic inhibitions (*knl-1*, *CENP-C^{hcp-4}*, *hcp-1/2* and *zyg-9* RNAi). Images are a partial z stack projection; arrowheads denote misaligned chromosomes. Bar, 2 μm .

(D) Quantification of the number of phospho-H3S10 positive nuclei upon inhibition of mitosis in the distal germline. Experimental scheme is the same as is presented in *Fig. 1B*, but instead of live imaging, gonads were extruded, fixed and stained. Error bars are SEM; unpaired *t* test shows high significance ($p<0.001$) between control and each individual inhibition.

(E) DAPI-stained nuclei in *zyg-1^{ts}* germlines 24h post upshift of L4 larvae showing the presence of micronuclei. Image 1 is from the mitotic zone, image 2 the transition zone and images 3 and 4 pachytene. Bar, 2 μm .

Figure S2. Disruption of mitotic cell divisions does not affect meiotic entry or nuclear travel through the germline.

(A) Immunofluorescence images and quantification of extruded gonads 24h post upshift stained with DAPI and phospho-SUN-1S8; asterisk denotes the distal end of the gonad. Bar, 5 μm . Error bars are SEM; unpaired *t* test shows no significance ($p=0.34$) for the number of rows prior to uniform phospho-SUN-1S8 staining and mild significance ($p=0.01$) for the number of rows positive for phospho-SUN-1S8 between control and *zyg-1^{ts}* worms.

(B) Images of extruded gonads 48h post upshift of L4 larvae stained with DAPI to visualize overall germline morphology. Images are partial z stack projections; asterisk denotes the distal end of the gonad and dotted white boxes outline the transition zone. Bar, 10 μm . Quantification of the number of nuclear rows in the transition zone based on nuclear morphology. Error bars are SEM; unpaired *t* test shows no significance between control and *zyg-1^{ts}* worms, $p=0.78$.

(C) Immunofluorescence images of the pachytene region of extruded gonads stained for DNA and HTP-3 24h post upshift; partial z stack projections, arrow denotes an abnormal nucleus positive for HTP-3. Bar, 2 μm .

(D) Schematic of the experimental procedure for data presented in E and F. Injection of Cy3-dUTP was done as previously described [S1].

(E) Quantification of the position of Cy3-dUTP labeled nuclei in both control and *zyg-1^{ts}* for two different timepoints to assay nuclear travel. One set of worms was analyzed 0-2 hours after injection with no upshift and the other set was analyzed 24-26 hours after injection and upshift. The number of labeled nuclei was counted in each of the 5 different zones (MZ=mitotic zone; TZ/EP=transition zone/early pachytene; MP=mid-pachytene; LP/D=late pachytene/diplotene; Dia=diakinesis) and averaged for 10 worms per genotype. Error bars are SEM.

(F) Representative immunofluorescence images for the data presented in (E) for the 24-26 hour timepoint, counterstained with DAPI. Images are a maximum projection z stack, asterisk denotes the distal end of the gonad. Bar, 10 μ m.

Figure S3. Inhibition of ZYG-1 results in mild pairing and synapsis defects.

(A) Immunofluorescence images of fixed, extruded gonads 24h post upshift (mid-to-late pachytene stage) stained with HTP-3, SYP-1 and DAPI. Dotted white boxes highlight single, unsynapsed chromosomes. Bar, 1 μ m.

(B) Fixed, extruded gonads 24h post upshift analyzed by FISH using a 5S rDNA probe (which labels Chr V) and counterstained with DAPI. Top images show the distal gonad, at the region between the end of the mitotic zone (MZ) and the beginning of the transition zone (TZ). Bottom images show mid-to-late pachytene (MP/LP) stage nuclei; arrows indicate nuclei with more than one focus. Bar, 5 μ m. Shown below the images is quantification of the average number of foci in the region between the end of the mitotic zone and the beginning of the transition zone (MZ/TZ) and the mid-to-late pachytene stage (MP/LP); at least 10 worms per genotype were analyzed. The results show that at the border between the MZ and the TZ, there is no significant defect in pairing between the control and the *zyg-1^{ts}*

worms. In pachytene (MP/LP stage), nuclei with extra foci are observed. The presence of an extra focus could represent unpaired homologous chromosomes or extra chromosomal copies in a nucleus formed following a defective mitosis (aneuploidy). Based on the lack of a global effect of ZYG-1 inhibition on pairing and synapsis (e.g., see images in (A) and quantification of MZ-TZ border), we favor the interpretation that the extra foci reflect aneuploidy.

(C) Quantification of cell death seen following inhibition of the synapsis checkpoint. PCH-2, a AAA+-type ATPase, is a key component of this pathway. Data for control and *zyg-1^{ts}* is the same as in *Fig. 4A*. Error bars are SEM; unpaired *t* test shows mild significance ($p=0.035$) between *zyg-1^{ts}* alone and the double mutant.

Figure S4. Cell death in response to errors in mitosis protects against the formation of aneuploid gametes that fail to support embryonic development.

(A) Quantification of the number of phospho-H3S10 positive nuclei following inhibition of *spo-11* in both control and *zyg-1^{ts}* 24h post upshift. Error bars are SEM; unpaired *t* test shows no significant difference ($p=0.27$) between *zyg-1^{ts}* alone and the double mutant.

(B) Mid-to-late L4 worms of the indicated genotypes were shifted to a semi-permissive temperature (18.5°C) for 72 hours. Ten worms per genotype were singled and passed onto new plates every 24 hours. Plates were analyzed 24 hours after removing the worm for each time point. The number of hatched and unhatched embryos was determined to calculate % embryonic lethality. Error bars are SEM.

SUPPLEMENTAL REFERENCES

- S1. Jaramillo-Lambert A, Ellefson M, Villeneuve AM and Engebrecht J (2007) Differential timing of S phase, X chromosome replication and meiotic prophase in the *C. elegans* germ line. *Developmental Biology* 308:206-21.